Sustainable Energy & Fuels

Fluoroalkyl Ether-diluted Dimethyl Carbonate-based Electrolyte Solutions for High-voltage Operation of $LiNi_{0.5}Co_{0.2}Mn_{0.3}O_2$ Electrodes in Lithium Ion Batteries

Journal:	*Sustainable Energy & Fuels*
Manuscript ID	SE-ART-01-2018-000036.R1
Article Type:	Paper
Date Submitted by the Author:	02-Mar-2018
Complete List of Authors:	Doi, Takayuki; Doshisha University, Faculty of Science and Engineering Matsumoto, Ryo; Doshisha University, Faculty of Science and Engineering Cao, Ziyang; Doshisha University, Faculty of Science and Engineering Haruta, Masakazu; Doshisha University, Organization for Research Initiatives and Development Hashinokuchi, Michihiro; Doshisha University, Faculty of Science and Engineering Minoru, Inaba; Faculty of Science and Engineering, Doshisha University

Journal Name

ARTICLE

Received 00th January 20xx,
Accepted 00th January 20xx

DOI: 10.1039/x0xx00000x

www.rsc.org/

Fluoroalkyl Ether-diluted Dimethyl Carbonate-based Electrolyte Solutions for High-voltage Operation of $LiNi_{0.5}Co_{0.2}Mn_{0.3}O_2$ Electrodes in Lithium Ion Batteries

Takayuki Doi,* Ryo Matsumoto, Ziyang Cao, Masakazu Haruta, Michihiro Hashinokuchi, Minoru Inaba

The energy density of lithium-ion batteries can be increased by improving the battery voltage and/or specific capacity. However, conventional electrolyte solutions decompose oxidatively at high voltages. The stability against oxidation of electrolyte solutions could be enhanced by increasing the concentration of lithium salts. The nearly saturated 8.67 mol kg^{-1} $LiBF_4$/dimethyl carbonate (DMC) electrolyte solution enabled the high-voltage operation at 4.6 V of $LiNi_{0.5}Co_{0.2}Mn_{0.3}O_2$ positive-electrodes, and extended the discharge capacity to ca. 200 mAh g^{-1}. BF_4^- anions, as well as DMC solvents, were stabilized at the high concentration. To reduce the viscosity and Li concentration without losing the high stability against oxidation toward the practical use, the highly concentrated electrolyte solution was diluted with fluorinated co-solvents having a low donor ability. Raman spectroscopy revealed that the solvation structure of $LiBF_4$/DMC was maintained after the dilution with a specific fluoroalkyl ether. The resultant low-viscosity and -concentration electrolyte solution was highly stable against oxidation at the $LiNi_{0.5}Co_{0.2}Mn_{0.3}O_2$ electrodes as far as the DMC/$LiBF_4$ molar ratio is kept low. The charge/discharge performance was much better than that for a conventional 1 M $LiPF_6$/ethylene carbonate-based electrolyte solution and the energy density far exceeded that of 5-V class $LiNi_{0.5}Mn_{1.5}O_4$ electrodes.

Introduction

Lithium-ion batteries have greatly expanded their use since 1991 due to their high energy densities. Their performance still needs to be improved with regard to energy density, battery cycle life, rate capability, and safety to realize a smart community with highly-efficient energy utilization. The energy density of lithium-ion batteries (LIBs) can be increased by improving the battery voltage and/or specific capacity. Conventional positive-electrode materials used for LIBs, such as $LiMn_2O_4$ and $LiCoO_2$, work at potentials around 4.0 V vs. Li/Li$^+$, and deliver specific capacity about 140 mAh g^{-1}.[1-2] On the other hand, the working potentials of a graphite negative-electrode is already very low close to lithium metal and the specific capacity is more than 2.5 times higher than that of the conventional positive-electrodes.[3-4] Considering these facts, the improvement of positive electrodes, in terms of both working potentials and specific capacity, is particularly required for the performance improvement of LIBs. $LiNi_xMn_yCo_{(1-x-y)}O_2$, having a layered rock salt crystal structure, is one of the most promising active materials because it has considerable potential for delivering a high reversible capacity over 200 mAh g^{-1} by charging to high potentials above ca. 4.4 V.[5-12] However, the reversible capacity noticeably decreased upon repeated charge/discharge cycling in conventional electrolyte solutions used in commercial LIBs, i.e., ca. 1 mol dm^{-3} (= M) $LiPF_6$ dissolved in a mixture of ethylene carbonate (EC) and low-viscosity linear carbonates, such as dimethyl carbonate (DMC). The capacity fading is caused by the cracks of $LiNi_xMn_yCo_{(1-x-y)}O_2$ particles,[13-14] the phase transition of $LiNi_xMn_yCo_{(1-x-y)}O_2$ to spinel and/or rock salt structure,[15,16] and the oxidative decomposition of electrolyte solution.[17,18] The stability against oxidation of electrolyte solutions would be enhanced by controlling the solvation properties. Highly concentrated electrolyte solutions including solvent-in-salt electrolyte system are known to offer unique physicochemical properties such as a wide potential window owing to the enhanced stability against reduction and oxidation.[19-23] The enhancement of oxidative stability has been particularly noted for ether-[24,25] and carbonate ester-based[23] concentrated electrolyte solutions so far. A conventional carbonate ester-based 1 M $LiPF_6$/EC+DMC electrolyte solution contains ca. 12 solvent molecules per a lithium ion. Since a lithium ion is solvated with 4 solvent molecules in the first solvation shell, the residual 8 molecules are relatively free in the electrolyte solution.[26-30] The HOMO energy of a solvate EC molecule is lower than a free one,[31] and hence the former is expected to be more stable against oxidation than the latter. Therefore, if all EC molecules are bound to lithium ions, i.e., if an EC/Li molar ratio is less than 4, the stability of the electrolyte solution against oxidation should be enhanced. Unfortunately, however, the solubility of $LiPF_6$ in EC is not so high, while propylene carbonate (PC) and γ-butyrolactone (GBL)

Department of Molecular Chemistry and Biochemistry, Doshisha University, Kyotanabe, Kyoto 610-0321, Japan. E-mail: tdoi@mail.doshisha.ac.jp

† Electronic Supplementary Information (ESI) available. See DOI: 10.1039/x0xx00000x

dissolved much amount of lithium salts;[32] $LiPF_6$/PC, $LiBF_4$/PC and $LiBF_4$/GBL were nearly saturated at 4.45, 7.25 and 4.65 mol kg^{-1} at room temperature, which have a solvent/Li molar ratio of 2.20, 1.35 and 2.50, respectively.[33-36] We demonstrated that the highly concentrated PC-[33,34] and GBL-[35] based electrolyte solution exhibited high stability against oxidation at $LiNi_{0.5}Mn_{1.5}O_4$ electrodes. However, the increasing concentration resulted in a high viscosity and a cost increase through the use of much Li salts. These problems could be solved by diluting the highly concentrated electrolyte solution with appropriate solvents;[37-39] we previously reported that 33.3 vol.% of 1,1,2,2-tetrafluoroethyl-2,2,3,3-tetrafluoropropyl ether (HFE, $H(CF_2)_2CH_2OCF_2CF_2H$)-diluted solution, i.e., 2.50 mol kg^{-1} $LiBF_4$/PC+HFE (2:1 by vol.), was a reasonable compromise to attain a low viscosity (51.7 mPa s) and a low PC/Li molar ratio (2.39).[40] In fact, $LiNi_{0.5}Mn_{1.5}O_4$ positive-electrodes showed a good charge/discharge performance with low irreversible capacities in it. However, the viscosity and electrolyte concentration are still high, compared to those for the conventional electrolyte solution, and the further dilution was not allowed due to the low miscibility of HFE with $LiBF_4$/PC.

In the present work, DMC, which is less viscous than PC, was used as a main solvent for the preparation of highly concentrated electrolyte solutions.[23,41] The highly concentrated DMC-based electrolyte solution are resistant not to 5-V class $LiNi_{0.5}Mn_{1.5}O_4$ electrodes,[40] but to $LiNi_{0.5}Co_{0.2}Mn_{0.3}O_2$ electrodes which works at lower potentials. Then, two kinds of fluoroalkyl ether were employed as a diluent to reduce the high viscosity and concentration of the $LiBF_4$/DMC. The solvation structure of Li^+-DMC in the diluted electrolyte solutions was studied by Raman spectroscopy. Charge and discharge properties of $LiNi_{0.5}Co_{0.2}Mn_{0.3}O_2$ positive-electrodes was measured in the resultant electrolyte solution.

Experimental

Reagents and chemicals

$LiBF_4$ (Kishida Chemical), DMC (Kishida Chemical), HFE (Daikin Industries), and 1,1,2,2-tetrafluoroethyl-2,2,2-trifluoroethyl ether (TFEE, $HCF_2CF_2OCH_2CF_3$, Daikin Industries) were used without further purification. A given amount of $LiBF_4$ was dissolved in DMC to obtain $LiBF_4$/DMC with different concentrations ranging from 0.93 (ca. 1 M) to 8.67 mol kg^{-1} (nearly saturated), which correspond to DMC/Li molar ratios of from 11.8 to 1.28. A solvent mixture of DMC and HFE or TFEE was prepared at a given volume ratio, and then $LiBF_4$ was dissolved in them at a DMC/Li molar ratio of 3.00. As a result, 1.52 mol kg^{-1} $LiBF_4$/DMC+HFE (1:1), 0.73 mol kg^{-1} $LiBF_4$/DMC+HFE (1:2), and 1.55 mol kg^{-1} $LiBF_4$/DMC+TFEE (1:1) were obtained, which correspond to DMC/Li molar ratios of 3.00, 3.96 and 3.00, respectively. All the preparation of electrolyte solutions was conducted in an Ar filled glove box (DBO-1.5KP-DID, Miwa Mfg). 1 mol dm^{-3} $LiPF_6$/ethylene carbonate (EC) + diethyl carbonate (DEC) (1:1 by volume, Kishida Chemical) was used as a reference.

Characterization of electrolyte solution

The viscosities of the electrolyte solutions were measured with an Ubbelohde viscometer at room temperature in the Ar filled glove box. Raman spectra of the electrolyte solutions were recorded using a spectrometer (LabRAM HR Evolution, Horiba) equipped with a multichannel charge coupled device detector. The spectra were taken using a 785-nm laser (>100 mW) through an objective lens. The scattered light was collected in a backscattering (180◦) geometry for an integration time of 10 s × 30 times at room temperature.

Electrochemical measurements

Charge and discharge properties of $LiNi_{0.5}Co_{0.2}Mn_{0.3}O_2$-composite electrodes (NCM523) were investigated using two-electrode coin-type cells. The active material of $LiNi_{0.5}Co_{0.2}Mn_{0.3}O_2$ powder (Tanaka Chemical) was mixed with a conductor (10 wt%) and poly[(vinylidenefluoride)-co-chlorotrifluoroethylene] (P(VdF-CtFE)) (10 wt%) as a binder in 1-methyl-2-pyrrolidone to form a slurry. The conductor used was acetylene black (Denka) or graphitized Ketjenblack (FD-7001D, Lion Specialty Chemicals). The slurry was spread out onto an Al foil, and then dried at 80 ^{o}C for more than 18 h under vacuum. The NCM523 sheet was used as a working electrode. A counter electrode was a Li foil. Microporous polypropylene film (Celgard® 2400) and glass filter (GF/D, Whatman®) were used as a separator for EC+DEC- and DMC-based electrolyte solution, respectively. All the test cells were assembled in the Ar filled glove box with a dew point below -80 ^{o}C. Charge and discharge tests (TOSCAT-3100, Toyo System) were performed at 30 ^{o}C between 3.0 and 4.4, 4.6 or 4.8 V. A slow charge/discharge rate of C/10, so that each charge and discharge process should theoretically be completed in 10 h, was used in this study to emphasize the difference in the stability of the electrolyte solutions; the current density corresponds to ca. 120 μA cm^{-2}. At the intermissions between charging and discharging, the cells were rested under open circuit conditions for 1 h. The morphological changes of the NCM523 was observed by scanning electron microscopy (SEM) combined with energy dispersive X-ray spectrometry (EDX).

Results and discussions

Characterization of concentrated $LiBF_4$/DMC electrolyte solution

DMC was almost saturated at room temperature with 8.67 mol kg^{-1} $LiBF_4$, where the DMC/Li molar ratio is 1.28. This value was lower than those for the nearly saturated PC-based electrolyte solutions; PC/Li molar ratios of 4.45 mol kg^{-1} $LiPF_6$/PC and 7.25 mol kg^{-1} $LiBF_4$/PC are 2.20 and 1.35, respectively. Thus, more highly concentrated electrolyte solution was obtained with the use of DMC solvent. In addition, the viscosity of the nearly saturated 8.67 mol kg^{-1} $LiBF_4$/DMC (310 mPa s) was much lower than those for the nearly saturated 4.3 mol kg^{-1} $LiPF_6$/PC (706.5 mPa s) and 7.25 mol kg^{-1} $LiBF_4$/PC (3497 mPa s).[33,34]

Figure 1a shows Raman spectra of $LiBF_4$/DMC electrolyte solutions of different concentrations ranging from 1.11 to 8.67 mol kg^{-1}. A major peak at about 916 cm^{-1} was seen in a Raman spectrum of 1.11 mol kg^{-1} $LiBF_4$/DMC (DMC/Li^+ molar ratio=10.0), which is assigned to the O-CH_3 stretching vibration of free DMC molecules.[42-44] A weak shoulder assigned to DMC molecules solvating lithium-ions was also observed at around 934 cm^{-1}. As the concentration of $LiBF_4$ increased, free DMC (ca. 916 cm^{-1}) gradually

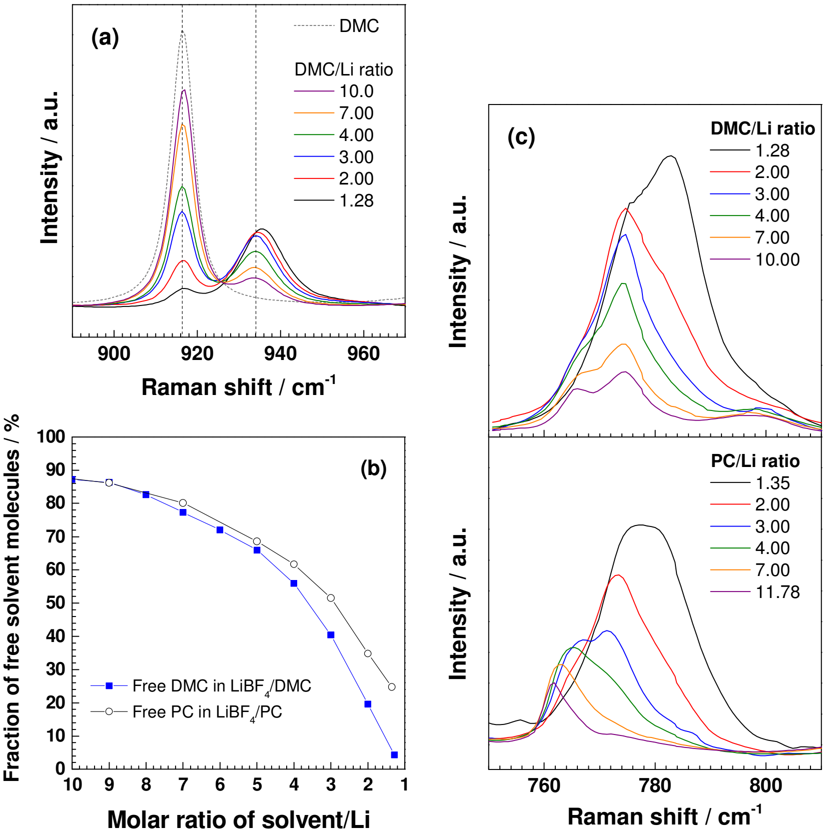

Figure 1. (a) Raman spectra of DMC and LiBF$_4$/DMC electrolyte solution of different DMC/Li molar ratios. (b) Relative area ratios (%) of Raman peaks assigned to free DMC at ca. 916 cm^{-1} and to solvating DMC at ca. 934 cm^{-1} in Figure 1a, and of those assigned to free PC at ca. 710 cm^{-1} and to solvating PC at ca. 720 cm^{-1} in Figure. 1 of ref.34. (c) Raman spectra of LiBF$_4$/DMC and LiBF$_4$/PC of different solvent/Li molar ratios.

decreased while solvating DMC (ca. 933 cm^{-1}) increased instead. The nearly saturated 8.67 mol kg^{-1} LiBF$_4$/DMC (DMC/Li$^+$=1.28) gave a major peak at around 936 cm^{-1}, suggesting that almost all of DMC molecules (96%) are bound to lithium ions. The relative area ratios of ca. 916- and 934-cm^{-1} peaks are summarized in Figure 1b, together with those of ca. 710- (free PC) and 720- (solvate PC) cm^{-1} peaks for LiBF$_4$/PC for comparison.[34,45] The fraction of free DMC molecules was smaller than that for free PC at a given solvent/Li molar ratio, which indicates that free solvent molecules can be effectively reduced in LiBF$_4$/DMC. One thing to note here is that the peak assigned to the B-F symmetric stretching vibration band (ca. 766 cm^{-1}) gradually shifted toward higher wavenumbers with an increase in the electrolyte concentration (Figure 1c); the bands at 766, 774, and 783 cm^{-1} were observed for LiBF$_4$/DMC, indicating an increase in the ionic association of LiBF$_4$ with increasing concentration.[46] These peaks were located at somewhat higher wavenumbers than those for the nearly saturated LiBF$_4$/PC and LiBF$_4$/acetonitrile (AN) solution.[34,46] These results suggest that the ionic association of LiBF$_4$ should be further enhanced in DMC, compared to PC and AN. DMC ($\varepsilon_r \approx 3$) has a much lower relative dielectric constant than PC ($\varepsilon_r \approx 65$) and AN ($\varepsilon_r \approx 36$), and hence Li$^+$, BF$_4^-$ and DMC molecules are more likely to form the aggregates, which should result in increasing the stability of BF$_4^-$, as well as DMC, against oxidation.

Effect of the LiBF$_4$ concentration in DMC on the stability against oxidation at NCM523

Charge/discharge properties of NCM523 was preliminarily investigated using a conventional electrolyte solution of 1 M LiPF$_6$/EC+DEC (1:1 by volume) in different voltage ranges to determine the targeted voltage range in this study.[8] The initial charge/discharge capacity of NCM523 increased as the charging cut-off voltage increased from 4.4 to 4.8 V (Figure S1a-c in Supporting Information), the values of which are summarized in Table S1. The capacity gradually faded with repeated charge/discharge cycling, and the capacity fading was more severe at the higher cut-off voltages.[8] As a result, the energy density at the 50th cycle, which was evaluated by integrating the discharge curve, was the highest when charge/discharge cycling was conducted between 3.0 and 4.6 V (Table S1d); the discharge capacity at the 50th cycle corresponded to 86.9% of the initial capacity. Hence, hereafter, we set the voltage range for charge/discharge measurements to 3.0-4.6 V.

Figure 2a, b and c show charge and discharge curves of Li|NCM523 cells using 0.93, 3.70 and 8.67 mol kg^{-1} LiBF$_4$/DMC, respectively, and the values are summarized in Table 1. The initial

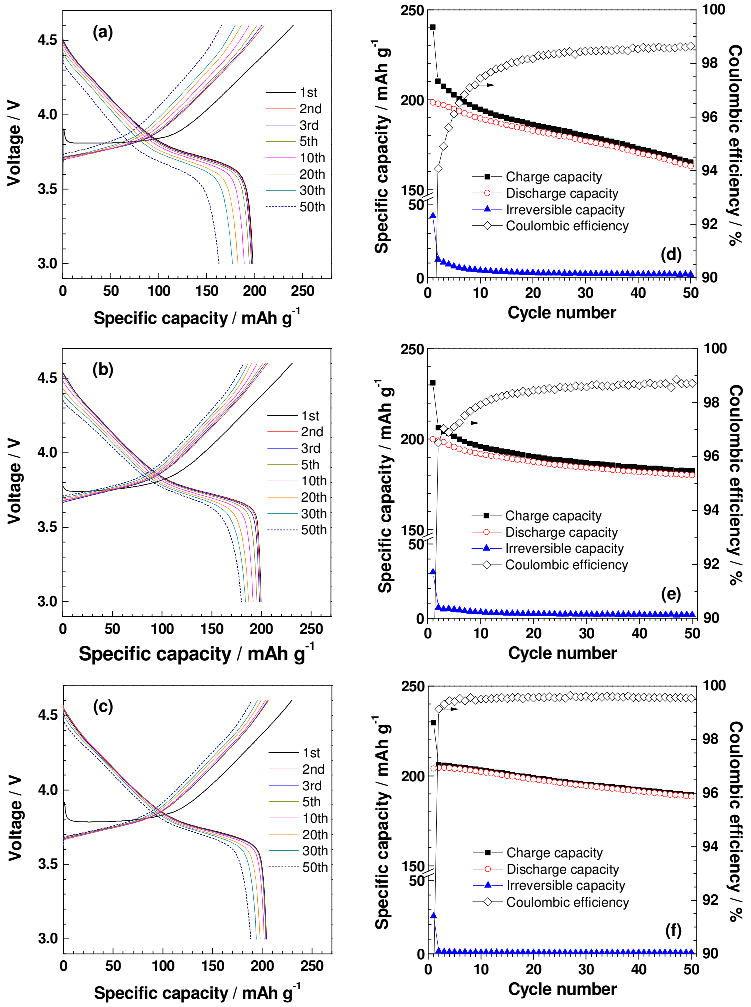

Figure 2. (a-c) Charge and discharge curves and (d-f) variations of capacities and Coulombic efficiency of Li|$LiNi_{0.5}Co_{0.2}Mn_{0.3}O_2$ cells with cycle number using (a and d) 0.93 mol kg^{-1} (ca. 1 M), (b and e) 3.70 mol kg^{-1}, and (c and f) nearly saturated 8.67 mol kg^{-1} $LiBF_4$/DMC.

Table 1. Charge, discharge, and irreversible capacities and Coulombic efficiency in the 1st cycle, and capacity retention at the 50th cycle of Li|$LiNi_{0.5}Co_{0.2}Mn_{0.3}O_2$ cells using 0.93, 3.70 and 8.67 mol kg^{-1} $LiBF_4$/DMC. The charging cut off voltage was 4.6 V.
[a] defined as percent ratios of discharge capacity in the 50th cycle to that in the 1st cycle.

$LiBF_4$/DMC		1st cycle				50th cycle
Concentration (mol kg^{-1})	DMC/Li molar ratio	Charge capacity (mAh g^{-1})	Discharge capacity (mAh g^{-1})	Irreversible capacity (mAh g^{-1})	Coulombic efficiency (%)	Capacity retention[a] (%)
0.93	11.8	240	199	41	82.6	82.2
3.70	3.00	231	200	31	86.5	90.0
8.67	1.28	230	204	26	88.9	92.2

discharge capacity of the NCM523 electrode reached 199 mAh g^{-1} in 0.93 mol kg^{-1} $LiBF_4$/DMC (DMC/Li^+ molar ratio=11.8). However, the initial irreversible capacity was very high, which resulted in a poor Coulombic efficiency (82.6%). These results suggest that irreversible reactions, such as the oxidative decomposition of the electrolyte solution, occurred at high potentials. Increasing $LiBF_4$ concentration in DMC resulted in a significant suppression of irreversible capacity and an improvement of Coulombic efficiency in the 1st cycle (Figure 2b and c, and Table 1). These results clearly indicate that the oxidative decomposition of electrolyte solution was

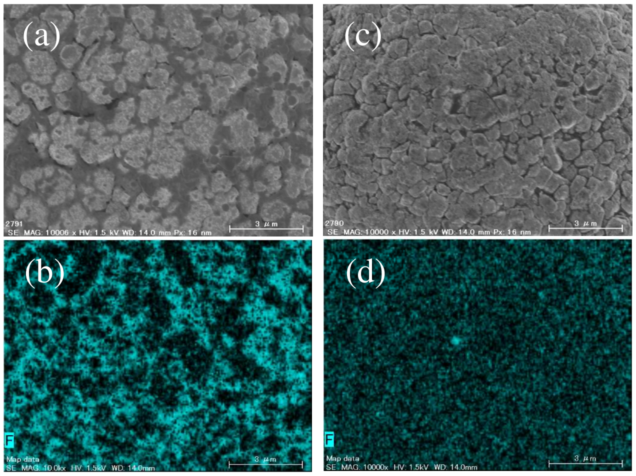

Figure 3. SEM/EDX images of $LiNi_{0.5}Co_{0.2}Mn_{0.3}O_2$ electrodes after 50 charge/discharge cycles between 3.0 and 4.6 V in (a and b) 0.93 mol kg^{-1} (ca. 1 M) and (c and d) nearly saturated 8.67 mol kg^{-1} $LiBF_4$/DMC.

effectively suppressed by employing the highly concentrated $LiBF_4$/DMC. The high Coulombic efficiency in the highly concentrated $LiBF_4$/DMC was kept over 50 charge/discharge cycles (Figure 2d and e). In 3.70 (DMC/Li^+=3.00) and 8.67 mol kg^{-1} $LiBF_4$/DMC (DMC/Li^+=1.28), high discharge capacities more than 180 mAh g^{-1} was maintained even at the 50th cycle, which corresponded to ≥ 90 % of the initial discharge capacity. These values were much higher than those obtained for 0.93 mol kg^{-1} $LiBF_4$/DMC (Table 1) and 1 M $LiPF_6$/EC+DEC (Table S1), indicating that the cycle performance of NCM523 was greatly improved in the nearly saturated 8.67 mol kg^{-1} $LiBF_4$/DMC. Figure 3 shows SEM/EDX images of NCM523 electrodes after the 50th cycle in 0.93 mol kg^{-1} and 8.67 mol kg^{-1} $LiBF_4$/DMC. A number of precipitates containing F were seen on the NCM523 electrode after charge/discharge cycling in 0.93 mol kg^{-1} $LiBF_4$/DMC (Figure 3a and b), indicating the oxidative decomposition of BF_4^- anions. The precipitates would interfere with lithium ion transfer reaction between NCM523 and electrolyte solution to degrade the charge/discharge performance. On the other hand, the formation of such F-containing precipitates was significantly suppressed in 8.67 mol kg^{-1} $LiBF_4$/DMC (Figure 3c and d). These results clearly indicate that BF_4^- anions are more stable against oxidation in the highly concentrated electrolyte solution, which is consistent with the Raman spectra in Figure 1c.

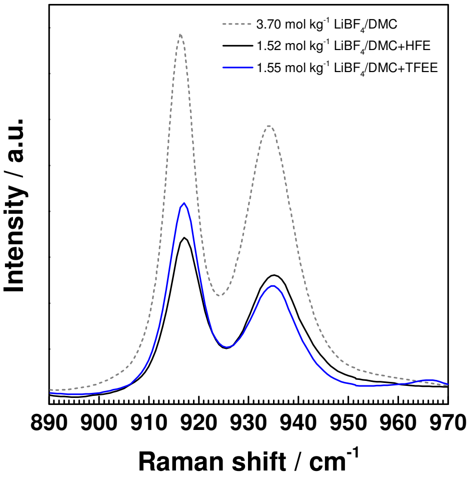

Figure 4. Raman spectra of 3.70 mol kg^{-1} $LiBF_4$/DMC, 1.52 mol kg^{-1} $LiBF_4$DMC+HFE (1:1) and 1.55 mol kg^{-1} $LiBF_4$/DMC+TFEE (1:1).

Table 2. Relative area ratios (%) of Raman peaks assigned to free DMC at ca. 916 cm^{-1} and to solvating DMC at ca. 934 cm^{-1} in Figure 4.

	DMC/Li molar ratio	Free DMC	Solvate DMC
3.70 mol kg^{-1} $LiBF_4$/DMC	3.00	43.8	56.2
1.52 mol kg^{-1} $LiBF_4$/DMC+HFE	3.00	44.6	55.4
1.55 mol kg^{-1} $LiBF_4$/DMC+TFEE	3.00	55.8	44.2

Dilution of highly concentrated $LiBF_4$/DMC with fluoroalkyl ether

The viscosity of 8.67 mol kg^{-1} $LiBF_4$/DMC (310 mPa s) was still high for practical application. We previously reported that the highly concentrated $LiBF_4$/PC system can be diluted with fluoroalkyl ether to reduce the viscosity;[40] fluoroalkyl ether of HFE is hardly involved in solvation of Li^+, and serves just as a diluting solvent. As a result, we obtained 33.3 vol.% of HFE-diluted solution (2.50 mol kg^{-1} $LiBF_4$/PC+HFE (2:1)) as a compromise of an acceptably low PC/Li molar ratio (2.39) and a low viscosity (51.7 mPa s).[40] A Li|$LiNi_{0.5}Mn_{0.2}Co_{0.3}O_2$ cell with 2.50 mol kg^{-1} $LiBF_4$/PC+HFE (2:1) gave almost the same initial discharge capacity (198 mAh g^{-1}) as that for nearly concentrated 7.25 mol kg^{-1} $LiBF_4$/PC, and exhibited higher rate-capability than it (Figure S2). However, the ionic conductivity of 2.50 mol kg^{-1} $LiBF_4$/PC+HFE (2:1) remained at 0.58 mS cm^{-1} at 25 °C, which was about 10 times as low as that of conventional 1 M $LiPF_6$/EC+DMC electrolyte solution (Figure S3). The viscosity of a conventional 1 M $LiPF_6$/EC+DMC electrolyte solution is ca. 3 mPa s, and hence a further decrease in viscosity, as well as electrolyte concentration, is required for practical application. However, the further HFE-dilution resulted in increasing the PC/Li molar ratio due to the low miscibility between HFE and $LiBF_4$/PC, which impairs the stability against oxidation. In this work, we used two kinds of fluoroalkyl ether, including HFE, as a diluent for highly concentrated $LiBF_4$/DMC system. To obtain an electrolyte solution with acceptably low-viscosity, -concentration and -DMC/Li molar ratio, 3.70 mol kg^{-1} $LiBF_4$/DMC (DMC/Li molar ratio=3.00) was diluted with HFE. As a result, 50 vol.% of HFE-diluted solution, i.e., 1.52 mol kg^{-1} $LiBF_4$/DMC+HFE (1:1 by vol.), maintained the low DMC/Li ratio (3.00), and showed a low viscosity of 3.6 mPa s. The further dilution resulted in a decrease in the solubility and an increase in the DMC/Li molar ratio because HFE can hardly dissolved $LiBF_4$, and is less miscible with highly concentrated $LiBF_4$/DMC. In fact, the 67 vol.% of HFE-diluted solution (DMC:HFE=1:2) dissolved only 0.73 mol kg^{-1} $LiBF_4$, where the DMC/Li molar ratio rose to 3.96. Another fluoroalkyl ether of TFEE

(-15.26 eV) has a much lower HOMO energy than HFE (-13.91 eV), and hence the stability against oxidation is expected to be higher than HFE. As with HFE, TFEE can hardly dissolve LiBF$_4$. 1.55 mol kg^{-1} LiBF$_4$ was dissolved in a solvent mixture of DMC+TFEE (1:1), which has the same DMC/Li ratio of 3.00 as 1.52 mol kg^{-1} LiBF$_4$/DMC+HFE (1:1 by vol.). The viscosity of the resultant solutions was low around 3 mPa s.

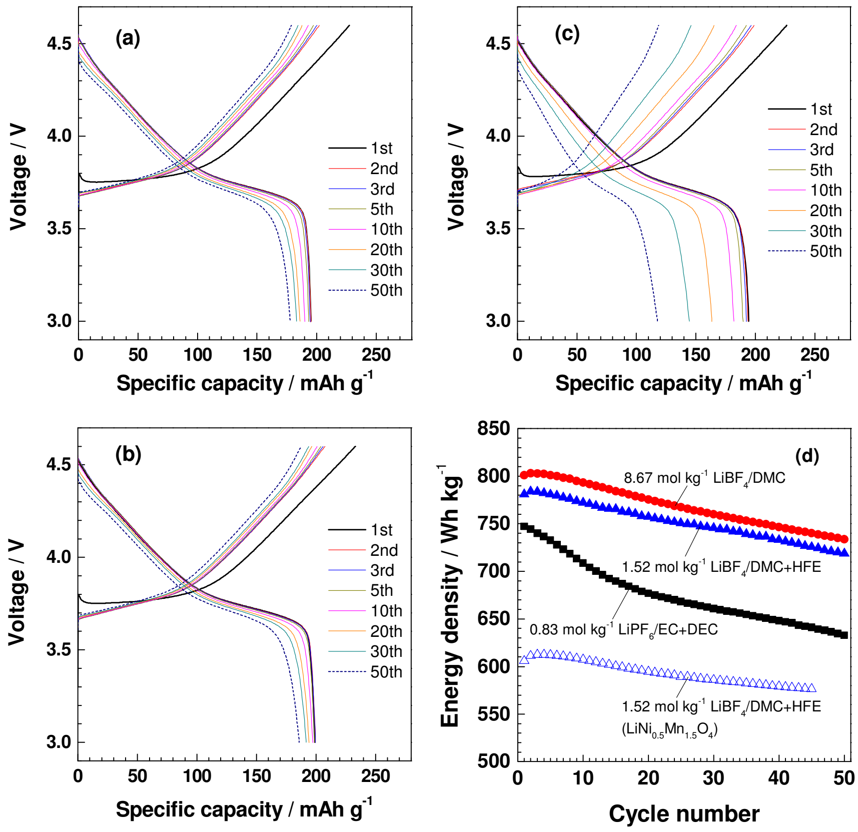

Figure 5. (a) Charge and discharge curves of Li|LiNi$_{0.5}$Co$_{0.2}$Mn$_{0.3}$O$_2$ cells using (a) 1.55 mol kg^{-1} LiBF$_4$/DMC+TFEE (1:1 by volume, DMC/Li ratio = 3.00), (b) 1.52 mol kg^{-1} LiBF$_4$/DMC+HFE (1:1 by volume, DMC/Li ratio = 3.00), (c) 0.73 mol kg^{-1} LiBF$_4$/DMC+HFE (1:2 by volume, DMC/Li ratio = 3.96). (d) Variation of energy density of LiNi$_{0.5}$Co$_{0.2}$Mn$_{0.3}$O$_2$ electrodes with cycle number, together with that of a LiNi$_{0.5}$Mn$_{1.5}$O$_4$ electrode in 1.52 mol kg^{-1} LiBF$_4$/DMC+HFE (1:1 by volume, DMC/Li ratio = 3.00) for comparison.

Charge/discharge performance of LiNi$_{0.5}$Mn$_{0.2}$Co$_{0.3}$O$_2$ electrodes in fluoroalkyl ether-diluted LiBF$_4$/DMC electrolyte solution

Figure 4 shows Raman spectra of 1.52 mol kg^{-1} LiBF$_4$/DMC+HFE (1:1) and 1.55 mol kg^{-1} LiBF$_4$/DMC+TFEE (1:1), together with 3.70 mol kg^{-1} LiBF$_4$/DMC, all of which have an equal DMC/Li molar ratio of 3.00. Relative area ratios of ca. 916- and 934-cm^{-1} peaks are summarized in Table 2. The fraction of free DMC molecules remained low in the HFE-diluted solution, while the dilution with TFEE resulted in a slight increase by about 10 %. These results indicate that TFEE is more involved in solvation of Li$^+$ than HFE, and therefore seem to be less suitable for a diluent. In fact, the capacity fading of NCM523 in the TFEE-diluted electrolyte solution (Figure 5a) was more noticeable than that for the HFE-diluted one (Figure 5b). The low charge/discharge performance would be associated with the large fraction of free DMC molecules and/or vulnerable TFEE to oxidation more than 4.5 V (Figure S4). On the other hand, in the HFE-diluted electrolyte solution, the initial discharge capacity and Coulombic efficiency were almost equal in both 1.52 mol kg^{-1} LiBF$_4$/DMC+HFE (1:1 by volume, DMC/Li molar ratio=3.00) and 0.73 mol kg^{-1} LiBF$_4$/DMC+HFE (1:2 by volume, DMC/Li ratio=3.96), as indicated in Figure 5b and c, respectively. A major difference was seen upon repeated charge/discharge cycling; the charge/discharge capacities considerably reduced in 0.73 mol kg^{-1} LiBF$_4$/DMC+HFE (1:2), while a relatively high discharge capacity (186 mAh g^{-1}), which corresponded to 93.4 % of the initial discharge capacity, was maintained even after 50 cycles in 1.52 mol kg^{-1} LiBF$_4$/DMC+HFE (1:1) (Figure 5b). The present results clearly show that highly concentrated LiBF$_4$/DMC system can be diluted with HFE without impairing the charge/discharge performance as long as the DMC/Li ratio is kept low (less than 3). Thus, low-viscosity and -concentration electrolyte solution with high stability against oxidation for NCM523 was developed. Finally, the discharge curves in Figure 5b were integrated by evaluating the energy density of NCM523. The energy density reached a maximum of 784 Wh kg^{-1}, which was comparable to that obtained for the nearly saturated 8.67 mol kg^{-1}

$LiBF_4$/DMC, and even higher than that for a conventional 1 M $LiPF_6$/EC+DEC. Moreover, 5-V class $LiNi_{0.5}Mn_{1.5}O_4$ electrodes could work between 3.0 and 5.0 V by substituting PC for DMC of 1.52 mol kg^{-1} $LiBF_4$/DMC+HFE (1:1). However, the energy density of the $LiNi_{0.5}Mn_{1.5}O_4$ electrode remained below 613 Wh kg^{-1}, as shown in Figure 5d. Thus, NCM523 far exceeded $LiNi_{0.5}Mn_{1.5}O_4$ in energy density.

Conclusions

DMC was almost saturated at room temperature with $LiBF_4$ at very high concentration of 8.67 mol kg^{-1}. The BF_4^- anions, as well as DMC, were stabilized against oxidation in the highly concentrated $LiBF_4$/DMC. As a result, 8.67 mol kg^{-1} $LiBF_4$/DMC enabled high-voltage operation of NCM523 electrodes, and greatly improved the charge/discharge performance of NCM523. The highly concentrated $LiBF_4$/DMC could be diluted with a specific fluoalkyl ether (HFE) without impairing the charge/discharge performance; 50 vol.% of HFE-diluted solution, i.e., 1.52 mol kg^{-1} $LiBF_4$/DMC+HFE (1:1), satisfied low-viscosity, -concentration, and -DMC/Li molar ratio, and elicited a high discharge capacity of ca. 200 mAh g^{-1} by charging the NCM523 electrodes to 4.6 V. The improved charge/discharge performance was maintained even after 50 charge/discharge cycles, which was comparable to that obtained for the nearly saturated 8.67 mol kg^{-1} $LiBF_4$/DMC, and even better than that for a conventional 1 M $LiPF_6$/EC+DEC electrolyte solution. The energy density of NCM523 reached a maximum of 784 Wh kg^{-1}, and far exceeded that of 5-V class $LiNi_{0.5}Mn_{1.5}O_4$. Thus, the electrolyte solution developed in this study possessed high stability against oxidation, low-viscosity, and relatively low concentration. However, it is volatile (Figure S5) and the Li concentration of 1.52 mol kg^{-1} $LiBF_4$ is still a little high, as compared with the conventional electrolyte solution, and volatile Diluents with the higher miscibility and stability against oxidation are required for realizing a $LiBF_4$/DMC-based electrolyte solution to be used in practical LIBs.

Conflicts of interest

There are no conflicts to declare.

Acknowledgements

The authors thank Dr. Katsuyuki Takahashi, Ms. Hiroe Nakagawa, and Mr. Shuji Hitomi, Dr. Tokuo Inamasu in GS Yuasa International Ltd. for their helpful discussion. This research was partially supported by "the Super Cluster Program" from MEXT and JST and "Kyoto Regional Scientific Innovation Hub" from MEXT.

References

1 J. M. Tarascon, E. Wang, F. K. Shokoohi, W. R. McKinnon and S. Colson, The Spinel Phase of $LiMn_2O_4$ as a Cathode in Secondary Lithium Cells, *J. Electrochem. Soc.*, 1991, **138**, 2859−2864.

2 T. Ohzuku, A. Ueda, M. Nagayama, Y. Iwakoshi and H. Komori, Comparative study of $LiCoO_2$, $LiNi_{12}Co_{12}O_2$ and $LiNiO_2$ for 4 volt secondary lithium cells, *Electrochim. Acta*, 1993, **38**, 1159−1167.

3 R. Fong, U. von Sacken and J. R. Dahn, Studies of lithium intercalation into carbons using nonaqueous electrochemical cells, *J. Electrochem. Soc.*, 1990, **137**, 2009−2013.

4 S. Flandrois, B. Simon, Carbon materials for lithium-ion rechargeable batteries, *Carbon*, 1999, **37**, 165−180.

5 Z. Liu, A. Yu and J. Y. Lee, Synthesis and characterization of $LiNi_{1-x-y}Co_xMn_yO_2$ as the cathode materials of secondary lithium batteries, *J. Power Sources*, 1999, **81–82**, 416-419.

6 T. Ohzuku and Y. Makimura, Layered lithium insertion material of $LiCo_{1/3}Ni_{1/3}Mn_{1/3}O_2$ for lithium-ion batteries, *Chem. Lett.*, 2001, **30**, 642−643.

7 H. Zheng, Q. Sun, G. Liu, X. Song and V. S. Battaglia, Correlation between dissolution behavior and electrochemical cycling performance for $LiNi_{1/3}Co_{1/3}Mn_{1/3}O_2$–based cells, *J. Power Sources*, 2012, **207**, 134–140.

8 S.-K. Jung, H. Gwon, J. Hong, K.-Y. Park, D.-H. Seo, H. Kim, J. Hyun, W. Yang and K. Kang, Understanding the degradation mechanisms of $LiNi_{0.5}Co_{0.2}Mn_{0.3}O_2$ cathode material in lithium ion batteries, *Adv. Energy Mater.*, 2014, **4**, 1300787.

9 W. Liu, P. Oh, X. Liu, M.-J. Lee, W. Cho, S. Chae, Y. Kim and J. Cho, Nickel-rich layered lithium transition-metal oxide for high-energy lithium-ion batteries, *Angew. Chem., Int. Ed.*, 2015, **54**, 4440–4457.

10 J. Zheng, W. H. Kan and A. Manthiram, Role of Mn content on the electrochemical properties of nickel-rich layered $LiNi_{0.8-x}Co_{0.1}Mn_{0.1+x}O_2$ ($0.0 \leq x \leq 0.08$) cathodes for lithium-ion batteries, *ACS Appl. Mater. Interfaces*, 2015, **7**, 6926–6934.

11 J. W. Choi and D. Aurbach, Promise and reality of post-lithium-ion batteries with high energy densities, *Nat. Rev. Mater.*, 2016, **1**, 16013.

12 W. Li, B. Song and A. Manthiram, High-voltage positive electrode materials for lithium-ion batteries, *Chem. Soc. Rev.*, 2017, **46**, 3006–3059.

13 E.-J. Lee, Z. Chen, H.-J. Noh, S. C. Nam, S. Kang, D. H. Kim, K. Amine and Y.-K. Sun, Development of microstrain in aged lithium transition metal oxides, *Nano Lett.*, 2014, **14**, 4873–4880.

14 K. Meng, Z. Wang, H. Guo, X. Li and D. Wang, Improving the cycling performance of $LiNi_{0.8}Co_{0.1}Mn_{0.1}O_2$ by surface coating with Li_2TiO_3, *Electrochim. Acta*, 2016, **211**, 822–831.

15 S.-U. Woo, C. S. Yoon, K. Amine, I. Belharouak and Y.-K. Sun, Significant improvement of electrochemical performance of AlF_3-coated $LiNi_{0.8}Co_{0.1}Mn_{0.1}O_2$ cathode materials, *J. Electrochem. Soc.*, 2007, **154**, A1005–A1009.

16 D. P. Abraham, R. D. Twesten, M. Balasubramanian, I. Petrov, J. McBreen and K. Amine, Surface changes on $LiNi_{0.8}Co_{0.2}O_2$ particles during testing of high-power lithium-ion cells, *Electrochem. Commun.*, 2002, **4**, 620–625.

17 M. Ue, M. Takeda, M. Takehara and S. Mori, Electrochemical properties of quaternary ammonium salts for electrochemical capacitors, *J. Electrochem. Soc.*, 1997, **144**, 2684–2688.

18 K. Xu, Nonaqueous liquid electrolytes for lithium-based rechargeable batteries, *Chem. Rev.*, 2004, **104**, 4303–4418.

19 Y. Hu, H. Li, X. Huang and L. Chen, Novel room temperature molten salt electrolyte based on LiTFSI and acetamide for lithium

batteries, *Electrochem. Commun.*, 2004, **6**, 28–32.

20 W. A. Henderson, F. McKenna, M. A. Khan, N. R. Brooks, V. G. Young and R. Frech, Glyme–lithium bis(trifluoromethanesulfonyl)imide and glyme–lithium bis(perfluoroethanesulfonyl)imide phase behavior and solvate structures, *Chem. Mater.*, 2005, **17**, 2284–2289.

21 L. Suo, Y.-S. Hu, H. Li, M. Armand and L. Chen, A new class of solvent-in-salt electrolyte for high-energy rechargeable metallic lithium batteries, *Nat. Commun.*, 2013, **4**, 1481.

22 Y. Yamada and A. Yamada, Review–superconcentrated electrolytes for lithium batteries, *J. Electrochem. Soc.*, 2015, **162**, A2406–A2423.

23 J. Wang, Y. Yamada, K. Sodeyama, C. H. Chiang, Y. Tateyama and A. Yamada, Superconcentrated electrolytes for a high-voltage lithium-ion battery, *Nat. Commun.*, 2016, **7**, 12032.

24 K. Yoshida, M. Nakamura, Y. Kazue, N. Tachikawa, S. Tsuzuki, S. Seki, K. Dokko and M. Watanabe, Oxidative-stability enhancement and charge transport mechanism in glyme-lithium salt equimolar complexes, *J. Am. Chem. Soc.*, 2011, **133**, 13121–13129.

25 C. Zhang, A. Yamazaki, J. Murai, J.-W. Park, T. Mandai, K. Ueno, K. Dokko and M. Watanabe, Chelate effects in glyme/lithium bis(trifluoromethanesulfonyl)amide solvate ionic liquids, part 2: importance of solvate-structure stability for electrolytes of lithium batteries, *J. Phys. Chem. C*, 2014, **118**, 17362–17373.

26 Y. Kameda, Y. Umebayashi, M. Takeuchi, M. A. Wahab, S. Fukuda, S.-I. Ishiguro, M. Sasaki, Y. Amo and T. Usuki, Solvation structure of Li^+ in concentrated $LiPF_6$-propylene carbonate solutions. *J. Phys. Chem. B*, 2007, **111**, 6104–6109.

27 M. D. Bhatt, M. Cho and K. Cho, Conduction of Li^+ cations in ethylene carbonate (EC) and propylene carbonate (PC): Comparative studies using density functional theory, *J. Solid State Electrochem.*, 2012, **16**, 435–441.

28 X. Bogle, R. Vazquez, S. Greenbaum, A. V. W. Cresce and K. Xu, Understanding Li^+–solvent interaction in nonaqueous carbonate electrolytes with ^{17}O NMR, *J. Phys. Chem. Lett.*, 2013, **4**, 1664–1668.

29 J. L. Allen, O. Borodin, D. M. Seo and W. A. Henderson, Combined quantum chemical/Raman spectroscopic analyses of Li^+ cation solvation: Cyclic carbonate solvents – Ethylene carbonate and propylene carbonate, *J. Power Sources*, 2014, **267**, 821–830.

30 I. Skarmoutsos, V. Ponnuchamy, V. Vetere and S. Mossa, Li^+ solvation in pure, binary, and ternary mixtures of organic carbonate electrolytes, *J. Phys. Chem. C*, 2015, **119**, 4502–4515.

31 M. D. Bhatt, M. Cho and K. Cho, Interaction of Li^+ ions with ethylene carbonate (EC): Density functional theory calculations, *Appl. Surf. Sci.*, 2010, **257**, 1463–1468.

32 M. Nie, D. P. Abraham, D. M. Seo, Y. Chen, A. Bose and B. L. Lucht, Role of Solution Structure in Solid Electrolyte Interphase Formation on Graphite with $LiPF_6$ in Propylene Carbonate, *J. Phys. Chem. C*, 2013, **117**, 25381–25389.

33 T. Doi, R. Masuhara, M. Hashinokuchi, Y. Shimizu and M. Inaba, Concentrated $LiPF_6$/PC electrolyte solutions for 5-V $LiNi_{0.5}Mn_{1.5}O_4$ positive electrode in lithium-ion batteries, *Electrochim. Acta*, 2016, **209**, 219–224.

34 T. Doi, Y. Shimizu, M. Hashinokuchi and M. Inaba, $LiBF_4$-based concentrated electrolyte solutions for suppression of electrolyte decomposition and rapid lithium-ion transfer at $LiNi_{0.5}Mn_{1.5}O_4$/electrolyte interface, *J. Electrochem. Soc.*, 2016, **163**, A2211–A2215.

35 T. Doi, Y. Shimizu, M. Hashinokuchi and M. Inaba, Low-viscosity γ-butyrolactone-based concentrated electrolyte solutions for $LiNi_{0.5}Mn_{1.5}O_4$ positive electrodes in lithium-ion batteries, *ChemElectroChem*, 2017, **4**, 2398–2403.

36 T. Doi, Y. Shimizu, R. Matsumoto, M. Hashinokuchi and M. Inaba, Suppression of Mn–ion–dissolution of $LiNi_{0.5}Mn_{1.5}O_4$ electrodes in a highly concentrated electrolyte solution at elevated temperatures, *ChemistrySelect*, 2017, **2**, 8824–8827.

37 K. Dokko, N. Tachikawa, K. Yamauchi, M. Tsuchiya, A. Yamazaki, E. Takashima, J.-W. Park, K. Ueno, M. Watanabe, S. Seki and N. Serizawa, Solvate ionic liquid electrolyte for Li-S batteries, *J. Electrochem. Soc.*, 2013, **160**, A1304–A1310.

38 N. Azimi, W. Weng, C. Takoudis and Z. Zhang, Improved performance of lithium-sulfur battery with fluorinated electrolyte, *Electrochem. Commun.*, 2013, **37**, 96–99.

39 M. Watanabe, M. L. Thomas, S. Zhang, K. Ueno, T. Yasuda and K. Dokko, Application of ionic liquids to energy storage and conversion materials and devices, *Chem. Rev.*, 2017, **117**, 7190–7239.

40 T. Doi, Y. Shimizu, M. Hashinokuchi and M. Inaba, Dilution of highly concentrated $LiBF_4$/propylene carbonate electrolyte solution with fluoroalkyl ethers for 5-V $LiNi_{0.5}Mn_{1.5}O_4$ positive electrodes, *J. Electrochem. Soc.*, 2017, **164**, A6412–A6416.

41 L. Doucey, M. Revault, A. Lautié, A. Chaussé and R. Messina, A study of the Li/Li^+ couple in DMC and PC solvents : Part 1: Characterization of $LiAsF_6$/DMC and $LiAsF_6$/PC solutions, *Electrochim. Acta*, 1999, **44**, 2371–2377.

42 J. E. Katon and M. D. Cohen, The vibrational spectra and structure of dimethyl carbonate and its conformational behavior, *Can. J. Chem.*, 1975, **53**, 1378–1386.

43 M. Morita, Y. Asai, N. Yoshimoto and M. Ishikawa, A Raman spectroscopic study of organic electrolyte solutions based on binary solvent systems of ethylene carbonate with low viscosity solvents which dissolve different lithium salts, *J. Chem. Soc. Faraday Trans.* 1998, **94**, 3451–3456.

44 H. Bohets, B. J. Van Der Veken, On the conformational behavior of dimethyl carbonate, *Phys. Chem. Chem. Phys.*, 1999, **1**, 1817–1826.

45 H. Tsunekawa, A. Narumi, M. Sano, A. Hiwara, M. Fujita and H. Yokoyama, Solvation and ion association studies of $LiBF_4$-propylenecarbonate and $LiBF_4$-propylenecarbonate-trimethyl phosphate solutions, *J. Phys. Chem. B*, 2003, **107**, 10962–10966.

46 D. M. Seo, O. Borodin, S.-D. Han, Q. Ly, P. D. Boyle and W. A. Henderson, Electrolyte solvation and ionic association I. Acetonitrile-lithium salt mixtures: Intermediate and highly associated salts, *J. Electrochem. Soc.*, 2012, **159**, A553–A565.

Journal Name

ARTICLE

Fluoroalkyl Ether-diluted Dimethyl Carbonate-based Electrolyte Solutions for High-voltage Operation of $LiNi_{0.5}Co_{0.2}Mn_{0.3}O_2$ Electrodes in Lithium Ion Batteries

Takayuki Doi,* Ryo Matsumoto, Ziyang Cao, Masakazu Haruta, Michihiro Hashinokuchi, Minoru Inaba

Table of contents

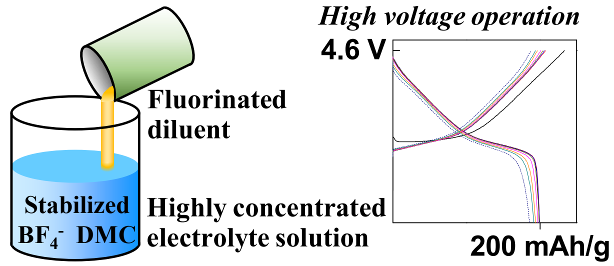

The high-voltage operation of $LiNi_{0.5}Co_{0.2}Mn_{0.3}O_2$ positive-electrodes is attained in highly concenrated $LiBF_4$/DMC electrolyte solution because of the stabilized BF_4^- and DMC molecules against oxidation, which should lead to improved energy density of lithium ion batteries.